

# Powered Descent Guidance Methods For The Moon and Mars

Ronald R. Sostaric \* and Jeremy R. Rea†

NASA Johnson Space Center, Houston, TX, 77058, USA

This study consists of a performance assessment of the various types of powered descent guidance methods previously used for missions to the Moon and Mars. The strengths and weaknesses of the various methods are discussed and simulation results are shown. Past methods have been used as a starting point for newer guidance schemes and one particular guidance scheme based on the Apollo Lunar Module Landing Guidance is discussed in greater detail. The guidance results are compared to optimal trajectory results, and a general outline for future powered descent trajectory guidance is suggested.

## Nomenclature

|                      |  |
|----------------------|--|
| $a$                  | Acceleration, m/s <sup>2</sup>   |
| $a_{cmd}$            | Commanded acceleration, m/s <sup>2</sup>                                       |
| $a_T$                | Total acceleration, m/s <sup>2</sup>   |
| $c_0, c_1, c_2$      | Unknown coefficients   |
| $d_1, d_2, d_3, d_4$ | Unknown coefficients   |
| $\vec{C}$            | Constraint vector(s)   |
| $D_N$                | Legendre psuedospectral differentiation matrix                                 |
| $g$                  | Acceleration due to gravity, m/s <sup>2</sup>                                  |
| $I_{sp}$             | Specific impulse, sec  |
| $L_{N-1}(t)$         | Legendre polynomial of order $N - 1$   |
| $L'_{N-1}(t)$        | First derivative of the Legendre polynomial                                    |
| $L/D$                | Lift-to-drag ratio   |
| $M_0$                | Initial mass, kg   |
| $M_f$                | Final mass, kg   |
| $M_p$                | Propellant mass, kg  |
| $R_x, R_y, R_z, r$   | Position, m  |
| $r_0$                | Initial position, m  |
| $r_t$                | Target position, m   |
| $t$                  | Time, sec  |
| $t_0$                | Initial time, sec  |
| $t_{go}$             | Time to go, sec  |
| $T/W$                | Thrust-to-Weight ratio   |
| $V_x, V_y, V_z, v$   | Velocity, m/s  |
| $v_0$                | Initial velocity, m/s  |
| $v_t$                | Target velocity, m/s   |
| $w_k$                | Weighting for Gaussian quadrature  |
| $\beta$              | Thrust heading angle in the horizontal plane measured CCW from the X-axis, deg |
| $\Delta V$           | Delta-V, m/s   |
| $\theta$             | Thrust angle from horizontal, deg  |

\*Aerospace Engineer, Flight Mechanics and Trajectory Design Branch, NASA Johnson Space Center, AIAA Senior Member.

†Aerospace Engineer, Flight Mechanics and Trajectory Design Branch, NASA Johnson Space Center, AIAA Member.

# Introduction

Successfully landing a spacecraft on a planetary surface requires some method to slow the descent rate of the vehicle and lessen the impact, such as parachutes, airbags, engine firings, or some combination. In particular, the use of rocket engine thrust to steer the vehicle to a soft landing allows for greater control during the descent and the ability to avoid hazards, such as rocks or craters. A trajectory guidance algorithm is also necessary to provide the thrust and attitude commands to deliver the vehicle to the surface safely. This algorithm must provide a trajectory that decreases the descent rate to an acceptable value while limiting the amount of propellant, and may also be required to achieve a certain landing accuracy and/or provide for hazard avoidance capability. The trajectory must also meet constraints on acceleration, attitude, and attitude rate.

## I. Powered Descent at the Moon

### A. Background

#### 1. Powered Descent Envelope

The powered descent is the final phase of flight leading to touchdown, and for that reason it is also sometimes referred to as “terminal” descent. Figure 1 shows an example Moon mission profile from the First Lunar Outpost study.<sup>1</sup> The sequence begins with a de-orbit burn, followed by a coast phase. Following the coast phase is the powered descent, which begins near periapse (or perilune) and terminates at touchdown.

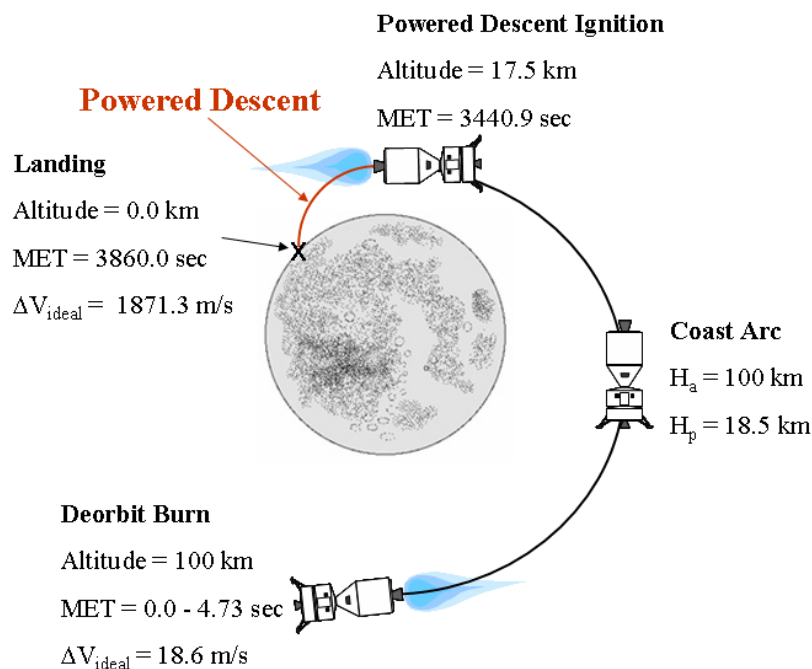


Figure 1. Example Moon Descent and Landing Profile

The powered descent itself may be broken into phases. Figure 2 shows an example of powered descent at the Moon. The longest phase is the initial braking phase. The throttle was designed to a constant 92% during this phase, to provide margin for potential throttle increases due to navigation updates. At 84 sec remaining, the braking phase ends and the pitch-up phase begins. During the pitch-up phase, a linear throttle down and linear pitch profile is commanded. At 24 sec remaining, the vehicle is directly above the landing site at an altitude of 100m. It then descends vertically at 33% throttle (1.2 Moon G's) to touchdown.

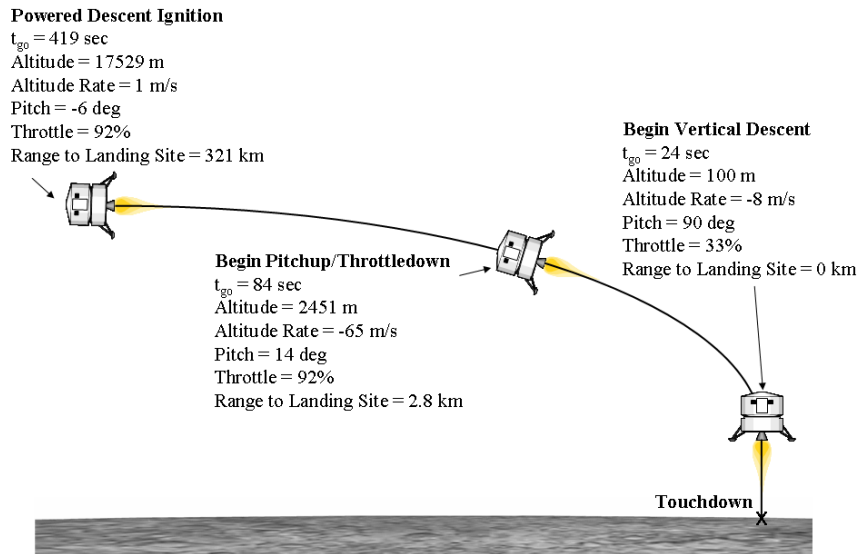


Figure 2. Example Moon Landing Powered Descent Trajectory

## 2. Apollo Lunar Descent Guidance

The Apollo Lunar Descent Guidance was designed to steer the vehicle from about 15 km altitude in an elliptical lunar orbit to the lunar surface. The guidance issued thrust and attitude commands given the vehicle state from the navigation routines.

The descent was broken into three separate phases (shown in Figure 3<sup>2</sup>):

1. Braking Phase (P63)
2. Approach Phase (P64)
3. Terminal Descent Phase (P66)

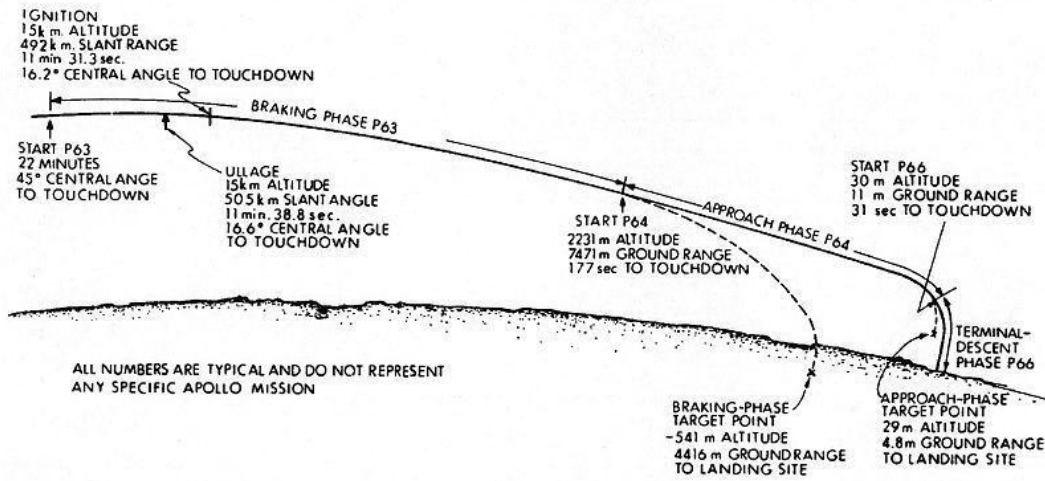


Figure 3. Apollo Lunar Descent Guidance Trajectory

The braking and approach phase each used the same guidance law, but the targets were different for each phase. The braking phase began at a slant range to target of 492 km. The transfer to the start of approach took about 514 sec and was near optimal. The target for the braking phase was a point below the surface and further downrange than the start of the approach phase.

The approach phase began with initial conditions of approximately 2.2 km altitude, 7.5 km ground range,

-44 m/s vertical velocity, and 129 m/s forward velocity. A typical approach phase took 146 sec. During this time the landing site could be manually re-designated. A target point was chosen that was not expected to be achieved, but would steer the vehicle to the desired point near to directly above the landing site with the desired conditions for P66 Terminal Phase start.

The algorithm designers were concerned with delay times due to computer processing, and derived the guidance law with a parameter to account for the delay. With current computing power, processing delay times are not a concern for this type of guidance algorithm. For a computational delay time of zero, the guidance equation (used for P63 and P64) reduced to:<sup>2</sup>

$$a_{cmd} = \frac{12(r_t - r)}{t^2} + \frac{6(v_t + v)}{t} + a_t \quad (1)$$

The terminal descent phase began at 30-m altitude and 11-m ground range from the target. During this phase, the vertical and horizontal velocity were controlled separately. The vertical guidance algorithm controlled the altitude rate by adjusting the throttle. The horizontal guidance algorithm nulled the horizontal velocity by making small changes to the thrust angle. It assumed the vertical component of thrust was constant. There was a 20° limit to the thrust angle during this phase.

The guidance operated in a surface-fixed coordinate frame with X-axis vertical, Z-axis in-plane and forward, and Y-axis completing the right hand coordinate system. Re-designation of the landing target (performed during the approach phase, if necessary) changed the origin of the coordinate system.

## B. Lunar Powered Descent Guidance Derivation and Simulation

The following guidance method was developed independently of the Apollo LM Guidance. However, the final result is similar to the explicit form of the Apollo LM Guidance law shown in equation (1).

### 1. Braking Phase

A powered descent trajectory at Moon typically begins with a long braking phase, designed to slow the vehicle velocity from orbital speeds. It can be shown, using optimal control theory, that the optimal steering law for this phase is the bilinear tangent law (if range is constrained):<sup>3</sup>

$$\tan \theta = \frac{d_1 t + d_2}{d_3 t + d_4} \quad (2)$$

where  $\theta$  is the thrust angle, and  $d_1$ ,  $d_2$ ,  $d_3$ , and  $d_4$  are unknown coefficients.

If range is not constrained, the steering law reduces to a single linear function, commonly known as the linear tangent law.

$$\tan \theta = d_1 t + d_2 \quad (3)$$

It is not possible, in general, to find a closed-form solution for the coefficients when solving this optimal control problem. Some methods have been developed to approximate the optimal solution.<sup>4</sup>

A simple method for calculating the trajectory is to develop an analytic profile that closely approximates the optimal solution. This can be accomplished by restricting the acceleration profile to a linear function in each axis.

$$a = c_1 + c_2 t \quad (4)$$

The acceleration profile is integrated to develop the analytic equations for velocity and position.

$$v = \int_{t_0}^t a = c_1(t - t_0) + \frac{1}{2}c_2(t - t_0)^2 + v_0 \quad (5)$$

$$r = \int_{t_0}^t v = \int_{t_0}^t \int_{t_0}^t a = \frac{1}{2}c_1(t - t_0)^2 + \frac{1}{6}c_2(t - t_0)^3 + v_0(t - t_0) + r_0 \quad (6)$$

The equations can be rewritten as follows,

$$tgo = t - t_0 \quad (7)$$

$$v_t - v_0 = c_1 t g_0 + \frac{1}{2} c_2 t g_0^2 \quad (8)$$

$$r_t - r_0 - v_0 t g_0 = \frac{1}{2} c_1 t g_0^2 + \frac{1}{6} c_2 t g_0^3 \quad (9)$$

In matrix form,

$$\begin{bmatrix} v_t - v_0 \\ r_t - r_0 - v_0 t g_0 \end{bmatrix} = \begin{bmatrix} t g_0 & \frac{1}{2} t g_0^2 \\ \frac{1}{2} t g_0^2 & \frac{1}{6} t g_0^3 \end{bmatrix} \begin{bmatrix} c_1 \\ c_2 \end{bmatrix}$$

Solve for the coefficients,  $c_1$  and  $c_2$ , by inverting the  $t g_0$  matrix.

$$\begin{bmatrix} c_1 \\ c_2 \end{bmatrix} = \begin{bmatrix} -\frac{2}{t g_0} & \frac{6}{t g_0^2} \\ \frac{6}{t g_0^2} & -\frac{12}{t g_0^3} \end{bmatrix} \begin{bmatrix} v_t - v_0 \\ r_t - r_0 - v_0 t g_0 \end{bmatrix}$$

In simplified form,

$$c_1 = \frac{-2(v_t + 2v_0)}{t g_0} + \frac{6(r_t - r_0)}{t g_0^2} \quad (10)$$

$$c_2 = \frac{6(v_t + v_0)}{t g_0^2} - \frac{12(r_t - r_0)}{t g_0^3} \quad (11)$$

The acceleration command is then given by

$$a_{cmd} = c_1 + c_2 t \quad (12)$$

The length of burn,  $t g_0$ , and position and velocity targets,  $r_0$  and  $v_0$ , respectively, must be provided. These targets are found using a combination of the “optimal” routines and trial and error from repeated simulation (Monte Carlo runs).

The following plots in figure 4 are an example nominal descent trajectory at the Moon using the scheme described above for the braking phase. Following the braking phase (which ends at  $t=3725.1$  sec), a quadratic acceleration scheme is used for the approach phase. The third and final phase is a vertical descent to the landing site at a constant acceleration. These phases are described further in the following sections.

The braking phase performance is dependent on the maximum engine thrust level. A series of simulations were run varying the maximum thrust for each run. The performance variation is shown in Figure 5 below. The minimum delta-V of about 1608 m/s occurs around an initial T/W = 0.55. The braking phase makes up the majority of the required delta-V for powered descent. More discussion of performance follows later in the “performance” section.

## 2. Quadratic Approach Phase

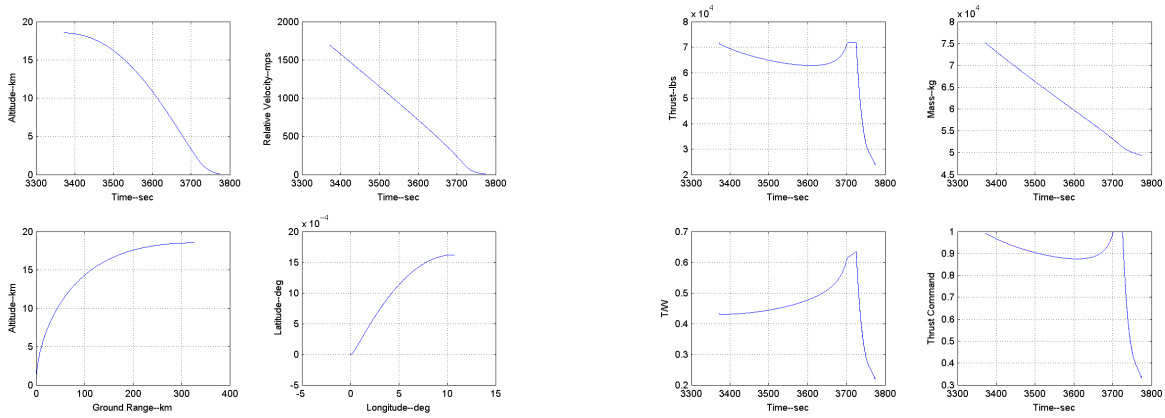
Following the braking phase, it is desirable to have a 2nd guidance phase which commands a pitch-over from the mostly horizontal attitude commanded during the braking phase to a vertical attitude in preparation for landing. During this time the engine will also be throttled down as the vehicle nears the surface. The throttle-down minimizes the disturbance of surface dust and allows for a less dynamic landing, as well protects for dispersions. This phase is called the “approach” phase, since the target will be directly above the landing site at some specified altitude with null horizontal velocity.

A simple method of calculating the thrust command for this phase is to restrict the acceleration profile to a quadratic equation of time.

$$a = c_0 + c_1 t + c_2 t^2 \quad (13)$$

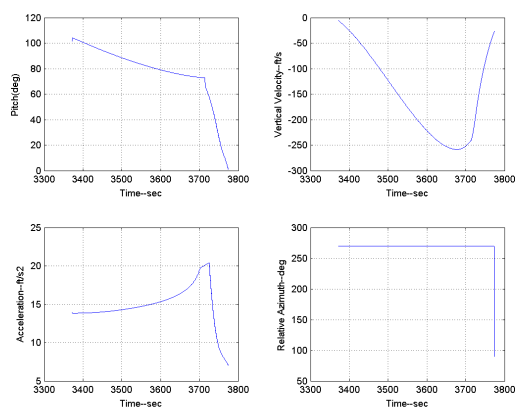
The acceleration profile is integrated to develop the analytic equations for velocity and position.

$$v = \int_{t_0}^t a = c_0(t - t_0) + \frac{1}{2} c_1(t - t_0)^2 + \frac{1}{3} c_2(t - t_0)^3 + v_0 \quad (14)$$

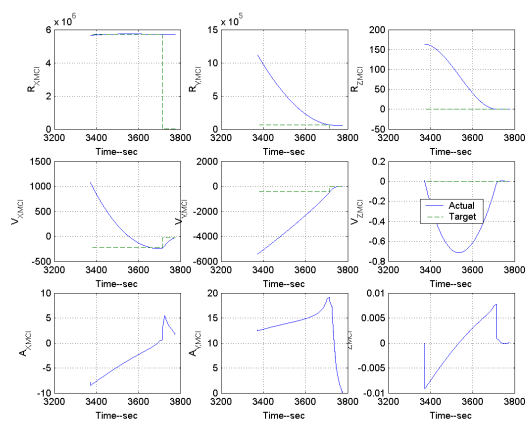


(a)

(b)



(c)



(d)

Figure 4. Simulated Guided Lunar Descent Trajectory

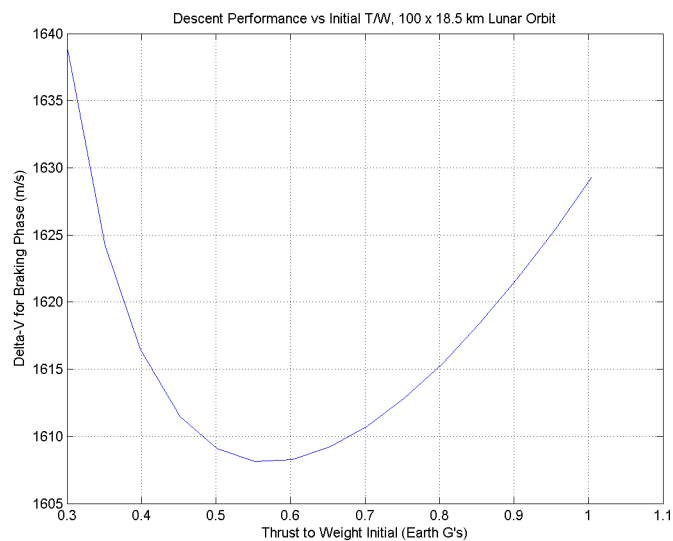


Figure 5. Braking Phase Performance Variation with T/W

$$r = \int_{t_0}^t v = \int_{t_0}^t \int_{t_0}^t a = \frac{1}{2}c_0(t-t_0)^2 + \frac{1}{6}c_1(t-t_0)^3 + \frac{1}{12}c_2(t-t_0)^4 + v_0(t-t_0) + r_0 \quad (15)$$

The equations can be rewritten as follows,

$$tgo = t - t_0 \quad (16)$$

$$a_t = c_0 + c_1tgo + c_2tgo^2 \quad (17)$$

$$v_t - v_0 = c_0tgo + \frac{1}{2}c_1tgo^2 + \frac{1}{6}c_2tgo^3 \quad (18)$$

$$r_t - r_0 - v_0tgo = \frac{1}{2}c_0tgo^2 + \frac{1}{6}c_1tgo^3 + \frac{1}{12}c_2tgo^4 \quad (19)$$

In matrix form,

$$\begin{bmatrix} a_t \\ v_t - v_0 \\ r_t - r_0 - v_0tgo \end{bmatrix} = \begin{bmatrix} 1 & tgo & tgo^2 \\ tgo & \frac{1}{2}tgo^2 & \frac{1}{3}tgo^3 \\ \frac{1}{2}tgo^2 & \frac{1}{6}tgo^3 & \frac{1}{12}tgo^4 \end{bmatrix} \begin{bmatrix} c_0 \\ c_1 \\ c_2 \end{bmatrix}$$

Solve for the coefficients,  $c_0$ ,  $c_1$ , and  $c_2$ , by inverting the  $tgo$  matrix.

$$\begin{bmatrix} c_0 \\ c_1 \\ c_2 \end{bmatrix} = \begin{bmatrix} 1 & -\frac{6}{tgo} & \frac{12}{tgo^2} \\ -\frac{6}{tgo} & \frac{30}{tgo^2} & -\frac{48}{tgo^3} \\ \frac{6}{tgo^2} & -\frac{24}{tgo^3} & \frac{36}{tgo^4} \end{bmatrix} \begin{bmatrix} a_t \\ v_t - v_0 \\ r_t - r_0 - v_0tgo \end{bmatrix}$$

Reducing into equation form,

$$c_0 = a_t - 6\frac{(v_t + v_0)}{tgo} + 12\frac{(r_t - r_0)}{tgo^2} \quad (20)$$

$$c_1 = -6\frac{a_t}{tgo} + 6\frac{(5v_t + 3v_0)}{tgo^2} - 48\frac{(r_t - r_0)}{tgo^3} \quad (21)$$

$$c_2 = 6\frac{a_t}{tgo^2} - 12\frac{(2v_t + v_0)}{tgo^3} + 36\frac{(r_t - r_0)}{tgo^4} \quad (22)$$

The length of burn,  $tgo$ , and position, velocity, and acceleration targets,  $r_t$ ,  $v_t$ , and  $a_t$ , respectively, must be provided. Typically, an altitude directly above the landing site is targeted, with zero horizontal velocity and a vertical orientation (zero horizontal acceleration). The vertical acceleration target is chosen to be equal to 1.2g, and is held constant through the 3rd and final “vertical” phase. The vertical velocity target is then determined from the vertical position and acceleration targets.

The above coefficients are computed at each guidance call, in each axis. The initial state for the two-point value boundary value problem is the current vehicle state (as estimated by the navigation algorithm). The targets for the final state typically do not change during the phase, unless a target re-designation is desired. The burn length to go,  $tgo$ , will decrease as the vehicle approaches the target state.

As  $tgo$  becomes very small the coefficient terms will tend toward infinity. There are typically two different methods employed to prevent this from happening. One method is to use a target state that forces the vehicle to follow the desired trajectory path without the intent of actually reaching that target. The guidance phase is then terminated prior to  $tgo$  approaching zero. The second method is to utilize the fine count, where the coefficients are not recalculated after  $tgo$  goes below a pre-selected value (typically 1-2 sec).

The acceleration command is then given by

$$a_{cmd} = c_0 + c_1t + c_2t^2 \quad (23)$$

At each guidance call, the coefficients are recalculated and  $t$  is set to zero. For  $t=0$ , the acceleration command is equal to  $c_0$ .

$$a_{cmd} = c_0 = a_t - 6 \frac{(v_t + v_0)}{t_{go}} + 12 \frac{(r_t - r_0)}{t_{go}^2} \quad (24)$$

This is the same result as the simplified version of the explicit equation used by the Apollo Lunar Descent Guidance in equation (1).

During the fine count, the coefficients are not recalculated, and  $t$  is not reset at each guidance call.

### 3. Vertical Phase

The vertical phase is the final guidance phase, ending at touchdown. During this phase, a vertical orientation is nominally commanded at a constant vertical acceleration. Current baseline lunar trajectories use a 100m altitude for the start of the phase and a 1.2g vertical acceleration throughout. This altitude allows time to divert to a different landing site in case of hazards.

If a secondary landing site is required, the vehicle still has the time before touchdown to achieve a new landing site with the necessary touchdown conditions (vertical orientation, low touchdown velocity). The nominal vertical phase begins at an altitude of 100 m and vertical velocity of -8.2 m/s (towards the surface). A constant thrust command of 0.3 brings the vehicle to the surface with a velocity of slightly greater than -1.0 m/s. The nominal vertical phase takes 20.9 sec and costs 40.9 m/s of delta-V.

An attempt was made to quantify the amount of time and delta-V that is necessary to perform a desired amount of divert. A series of cases with increasing divert was simulated. The pitch profile for these cases involved three segments of constant pitch rate. The first is a pitch over to a maximum of 25 deg, to start the vehicle in the desired direction of the divert. The second is a constant rate pitch over in the opposite direction (to a max of -25 deg), in order to null the vehicle horizontal velocity prior to touchdown. The final segment is a pitch over to 0 deg. The pitch rate for these cases was limited to 5 deg/sec. Also, the throttle rate was limited to 0.1 sec<sup>-1</sup>. The minimum throttle was set to 25%, with a max of 100%.

Table 1 shows the amount of extra time and delta-V that is required for the divert maneuver. Up to 50 m of divert can be performed at essentially no extra cost. The engine throttle is increased slightly to start the vehicle heading in the direction of the divert. It is then decreased slightly as the vehicle travels the desired divert distance. Then it is increased slightly to take the velocity back out. However, this does not impact the delta-V much since the average throttle is close to 0.3. Also note that the average descent rate is close to the nominal. Since most of the delta-V for this phase comes from gravity losses, the delta-V is very closely related to the length of the phase.

**Table 1. Divert Deltas From Nominal**

| Divert(m) | $\Delta$ Time (sec) | $\Delta$ Delta-V(m/s) |
|-----------|---------------------|-----------------------|
| 25.0      | -0.9                | -0.9                  |
| 50.0      | -0.6                | 0.6                   |
| 75.0      | 4.0                 | 8.2                   |
| 100.0     | 8.3                 | 15.5                  |
| 125.0     | 11.1                | 20.3                  |
| 150.0     | 15.4                | 27.4                  |

As divert distance is increased, the amount of extra time and delta-V is increased. It might be possible to further optimize the profile for these cases with larger number of segments in the pitch profile. However, this is the final phase right before touchdown, and every effort should be made to minimize the complexity and number of maneuvers at this stage of the flight. Thus, the simplest possible method (three segments only) was chosen.

Another method of performing the divert is selecting a new landing site earlier in the trajectory, during the approach phase. If this method is preferred, it may be advantageous to lower the start altitude of the vertical phase. During the Apollo missions, the landing site change was performed during the approach phase. The vertical phase started at an altitude of 30m above the surface. The horizontal velocity at the start of the vertical phase was not expected to be zero. No position constraint was enforced during this phase, only velocity constraints. It was called the Terminal Descent Phase, since a strictly vertical descent was not commanded.

#### 4. Performance

In order to determine the total performance for the Lunar Descent, the simulation was run from 100km circular orbit to the surface. A de-orbit burn was targeted for a 18.5 km perilune. The start of the braking phase burn was determined using NPSOL, an optimization code created at Stanford. The braking phase was performed using PEG, a variation of the Shuttle ascent guidance code, which provides a near optimal braking phase. This phase uses a max throttle burn. The PEG targets were also determined using the optimizer. Following the braking phase is a 60 sec pitch-over/throttle down phase. Both pitch over and throttle down are commanded at a constant rate for this phase. The phase targets a location 100-m directly above the landing site. The final vertical phase is a constant throttle descent, at a throttle setting determined using the optimizer. The end of phase target is less than 2 m/s velocity at touchdown.

Figure 6 shows the delta-V required for the entire descent as it varies with initial thrust-to-weight ratio. The minimum occurs at a initial T/W of 0.6. However, past experience has shown that overall system mass is optimized at a lower T/W. Figure 6 shows that the required delta-V does not increase rapidly until the T/W goes below 0.4. The amount of extra engine mass required to achieve T/W=0.6 tends to be greater than the extra propellant mass needed to meet the delta-V requirement for T/W=0.4, and so the overall optimal initial T/W is closer to 0.4.

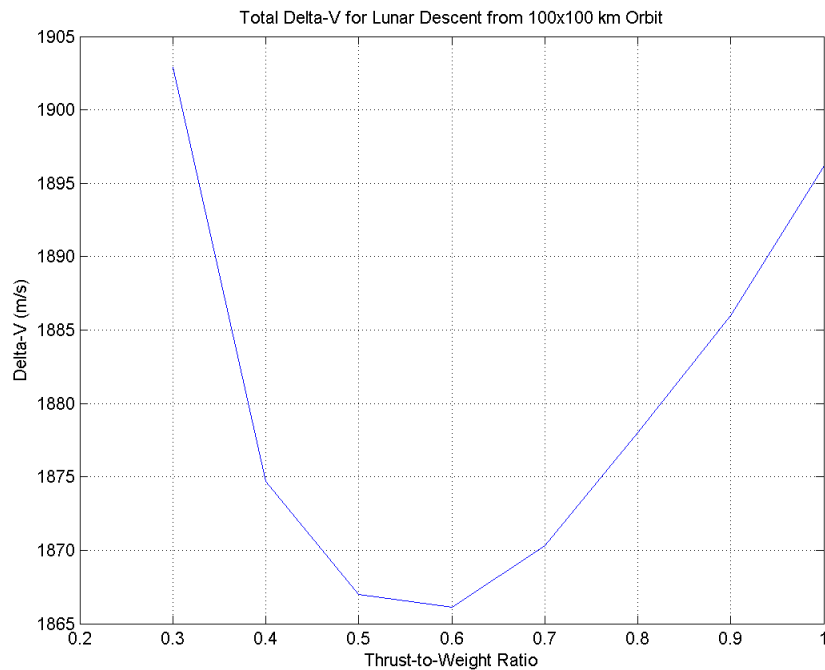


Figure 6. Total Delta-V Required for Lunar Descent from Parking Orbit

As a comparison, the Apollo powered descent phase needed about 2055 m/s of delta-V.<sup>1</sup> The primary reasons for the difference are that Apollo:

- Used a lower T/W (initial T/W  $\cong$  0.33)
- The total time of the burn was longer
- The engine could not throttle in the region between 65% and 92% throttle
- Had a surface viewing constraint

#### 5. Divert Out-of-Plane

Depending on the sensor suite and type of navigation algorithms employed for a Lunar Descent mission, the accuracy of the knowledge of the vehicle state may change quickly during flight. One navigation solution

being considered by engineers at the Johnson Space Center involves the use of a very accurate sensor with limited range. This sensor would be activated relatively close to the surface. It was determined that a near-worst case scenario would be to turn on the sensor only to discover that the vehicle was 2000 ft from the desired landing location in the out-of-plane direction. Navigation engineers were interested in understanding when this information must be available to guidance and control in order to still reach the target.

The trajectory shown in figure 4 was used as the nominal trajectory. The divert is commanded during the approach phase. If the divert is commanded at the start of approach, figure 7 shows that cost in delta-V is only a few m/s. As the time goes on and the vehicle nears the (soon to be realized as incorrect) target, the cost increases.

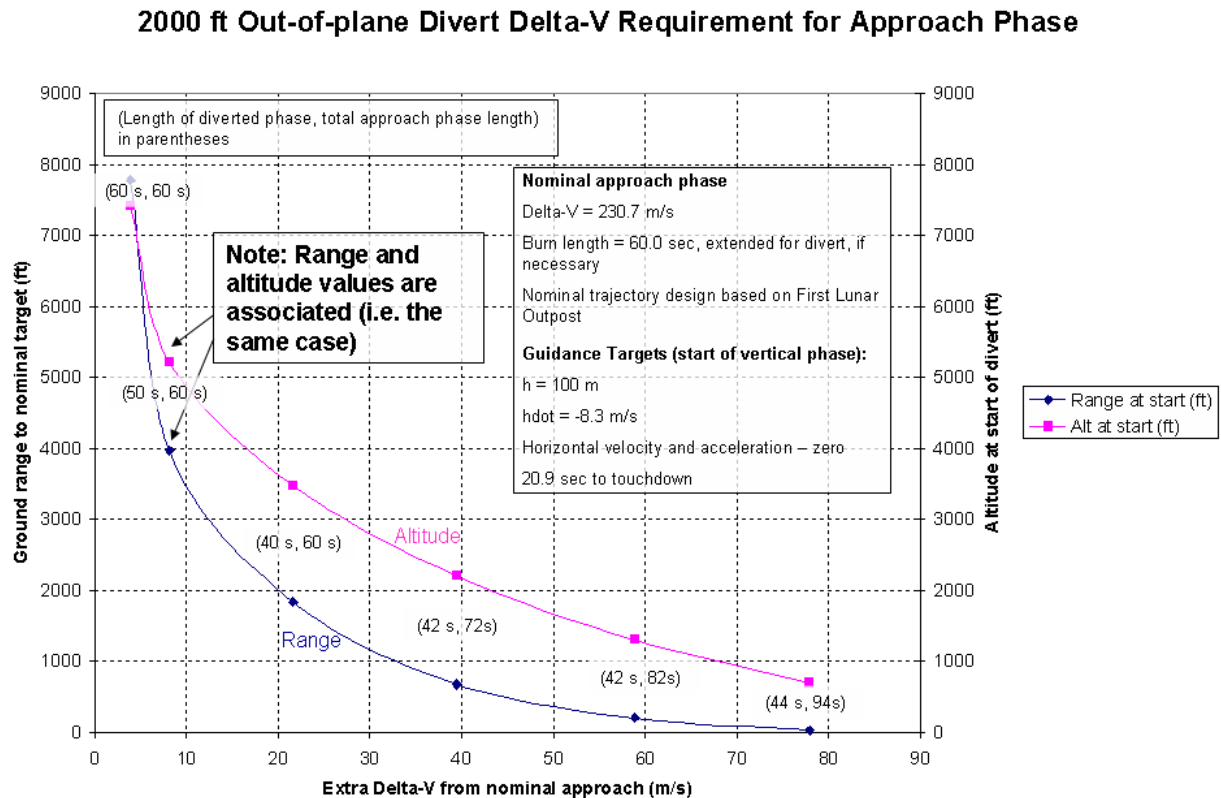


Figure 7. Out-of-Plane Divert Delta-V Requirements

Figure 7 shows both the altitude and range on the same plot using two different y-axes. The two curves are actually the same runs, one shows altitude and the other shows range.

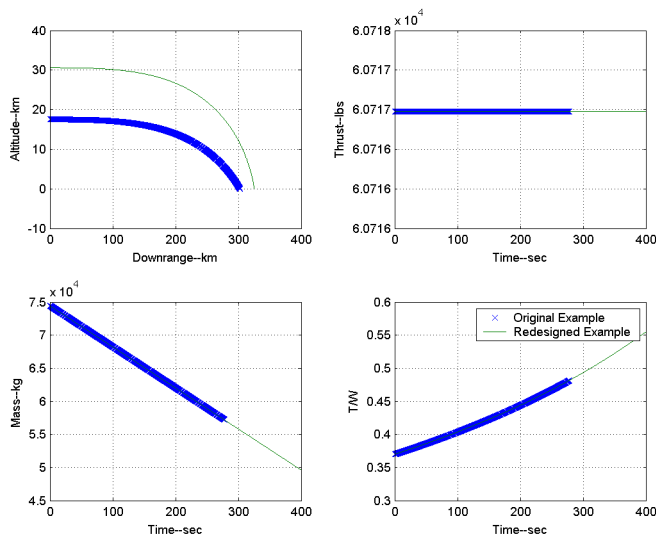
Note that the nominal approach phase delta-V is about 230 m/s. The results show that if you wait until 1000 ft altitude, you can still make the new target, but it costs about 70 m/s extra.

Cases were run every 10 sec from the start of the approach phase (from 0-50 sec after approach phase start). After about 20 sec, the delta-V starts to take off. For the 30 sec case and up, the total length of the approach phase was increased in order for the vehicle to make the target. The recommendation was not to wait much longer than 20 sec after the start of approach to make the decision for this kind of divert. The range to target at that point is 2000 ft, the altitude is about 3500 ft, and the extra cost in delta-V is about 22 m/s.

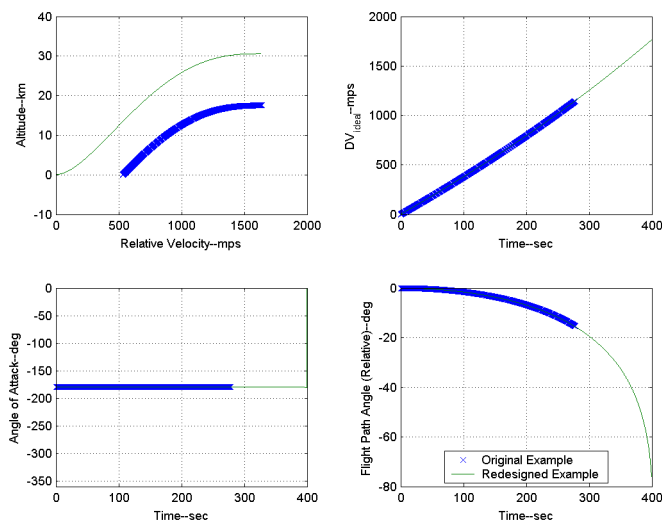
### C. Gravity Turn

Another type of powered descent method that is commonly used is gravity turn steering. Gravity turn steering requires that the thrust vector be oriented opposite to the instantaneous velocity vector during the descent.

The trajectory described in figure 2 can be modified to illustrate gravity turn steering. Starting at the same initial conditions depicted in figure 2, the gravity turn trajectory with a constant thrust was simulated, and is shown as the blue trajectory in figure 8. Note that this trajectory holds a  $-180$  deg angle of attack throughout. For this case, it takes approximately 280 sec to travel 300 km downrange and descend 17.5 km in altitude. Note in the flight path angle plot that the vehicle velocity vector is along the horizontal at the start of the trajectory, but is still traveling mostly horizontal (at  $-15$  deg) at touchdown. Also, note in the altitude-velocity plot (row 3, column 1) that the relative velocity at touchdown is still greater than 500 m/s. Clearly, this trajectory must be redesigned to something more reasonable. One simple solution is to start the gravity turn earlier, at a higher altitude.



(a)



(b)

**Figure 8. Redesigned Gravity Turn Trajectory**

Figure 8 shows the redesigned gravity turn (green line) in comparison to the trajectory above. The powered descent is initiated at a higher altitude (30.6 km). This would require starting the burn earlier along the “coast arc” depicted in figure 1, at a slightly slower velocity. It also would cause some impact to

the Earth-Moon transfer trajectory, but that will be neglected for the purposes of this example. Notice that the redesigned gravity turn achieves the small and nearly horizontal velocity required for safe touchdown.

The ideal delta-V for the gravity turn solution is 1716.5 m/s, compared to a delta-V of 1852.7 m/s for the solution with the pitch up maneuver depicted in figure 2. Since the gravity turn steering is thrusting opposite the velocity vector at all times, the velocity losses are minimized.

It is important to note that this “true” gravity turn method is only theoretical and could not be used as a guidance algorithm, because it can only meet final state constraints by adjusting the initial state, i.e. when you turn it on. However, modified versions of gravity turn guidance can and have been used successfully, in particular for the Viking program. Still, these types of algorithms have limitations. They are good at minimizing propellant usage but lack the landing precision and re-targeting capability of schemes similar to the Apollo LM Guidance.

## II. Powered Descent at Mars

Powered descent to the Martian surface presents a separate set of challenges than the Lunar descent. Due to the presence of an atmosphere, the powered descent at Mars is preceded by an atmospheric entry phase and a parachute phase, which slow the vehicle and reduce the velocity at the start of powered descent. At the Moon, the velocity at the start of powered descent is primarily horizontal. However, at Mars, the parachute removes most of the horizontal velocity, so the initial velocity is much more vertical. In order to minimize propellant, the engine should be ignited as late as possible and commanded at the highest setting. However, if the intent of the mission is to achieve an accurate landing, the powered descent must solve the remaining amount of position error, which can be substantial. Since earlier engine ignition is generally cheaper for flying large horizontal (“divert”) distances, this becomes a trade off. Past work has shown that conditions at the start of powered descent can vary widely, so this remains an interesting and challenging problem.

### A. Background

#### Viking Powered Descent Guidance

The Viking landers used a powered descent guidance scheme based on a gravity turn solution.<sup>5</sup> Due to wind and atmospheric variation at Mars, the velocity at the end of the parachute phase was expected to be in the range of 40-75 m/s vertical, and 0-80 m/s horizontal. The guidance scheme used two altitude-velocity reference profiles to attempt to bound the solution space—one high speed contour and one low speed contour. These were gravity turn solutions. Following this was a constant velocity phase that targeted 8 ft/s (2.44 m/s). This final phase began at an altitude of 16.8 m.

The engine was ignited at 1.5 km altitude, and after a 2 sec warm-up sequence the parachute was released. A pitch maneuver to the correct attitude was performed, then the H-V reference contour was commanded the rest of the way to the surface. Originally, the same H-V contour was followed for all cases, but it was discovered during simulation work that for the lower velocity cases the guidance would sometimes get behind the contour and end up impacting at a high velocity. This was the reason for the addition of the low velocity contour. For initial velocities between the two contours, interpolation was used to determine the H-V reference contour. For initial velocities outside of the range of the low and high speed contours, the nearest contour was used.

Figure 9 shows a reconstructed version of the Viking H-V contours. The simulation was set up using a gravity turn with constant thrust, starting at the initial conditions of the two contours. It was discovered that the H-V contour could be approximated extremely well using a third order function.

Low speed contour curvefit:

$$H = 3.06 * 10^{-7} + 1.53 * 10^{-1} * V + 8.795 * 10^{-5} * V^2 - 1.029 * 10^3 * V^3 \quad (25)$$

High speed contour curvefit:

$$H = 3.23 * 10^{-7} + 1.20 * 10^{-4} * V + 1.856 * 10^{-4} * V^2 - 2.479 * 10^4 * V^3 \quad (26)$$

Figure 10 shows a few other plots from the reconstructed trajectory. The plot in the top left corner shows the thrust command. The nominal thrust command for the high speed contour was about 0.64, and for the

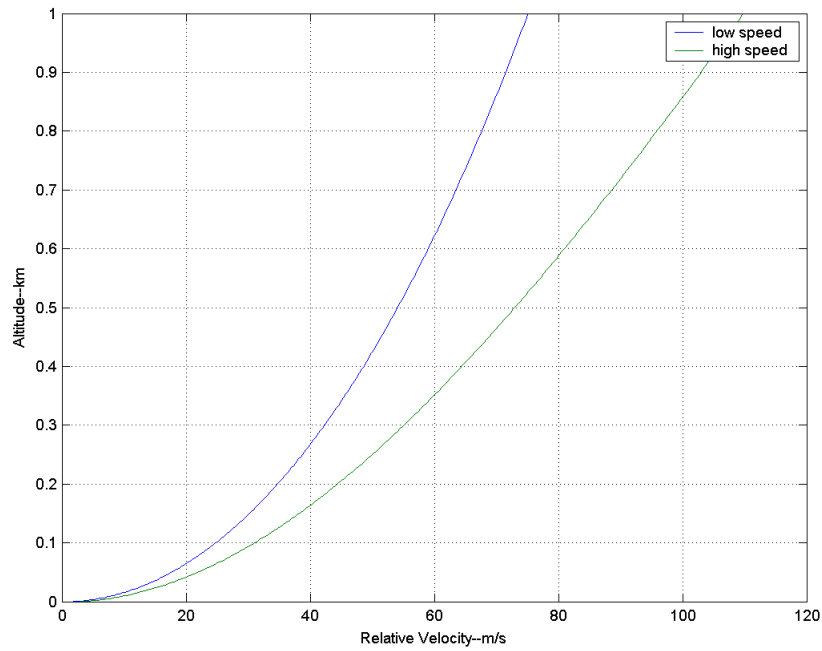


Figure 9. Viking H-V Contours

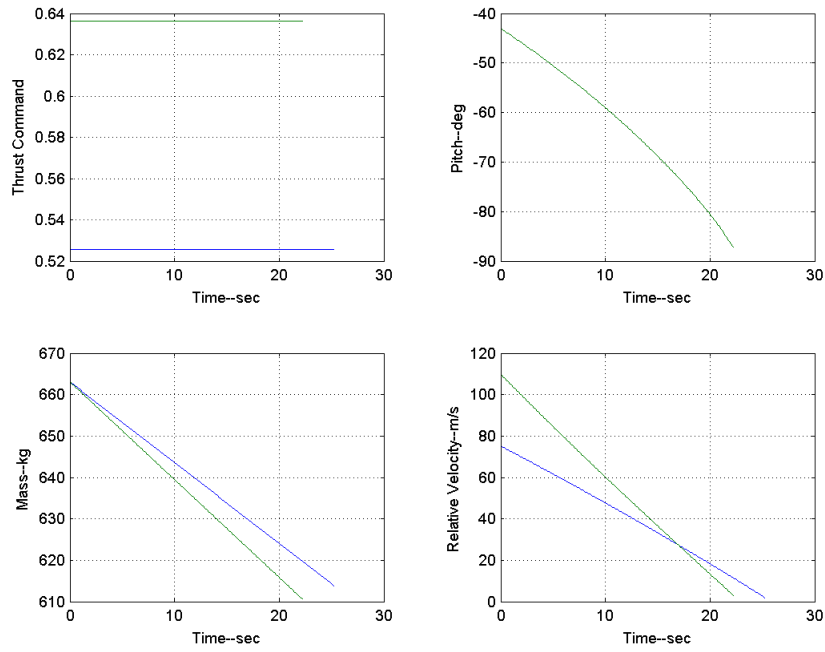


Figure 10. Viking Powered Descent Reconstructed Trajectory

low speed contour it was 0.53. Though designing to a higher thrust level would have saved some propellant mass, the designers chose to save some throttle capability to protect for dispersions.

Both the high speed and low speed contours start at the same altitude, but the low speed contour requires a lower thrust level, resulting in a longer burn than the higher thrust high speed contour.

The nominal required delta-V for this descent profile was 235 m/s.

## B. Pinpoint Landing

Future missions to Mars may require an accurate landing on the surface. The atmospheric entry phase can be guided accurately, given that the spacecraft has enough L/D during entry. However, limitations in knowledge of the vehicle state for the current state-of-the-art navigation sensor suites and algorithms show that substantial position error may still exist at the end of the entry phase<sup>7,8</sup>. Also, wind drift on a parachute may further increase position error from the desired landing site.

In order to achieve the desired landing position accuracy, the terminal descent system must be sized to be able to accommodate significant position errors at engine ignition. Past studies have shown that a single quadratic approach phase would use too much fuel to fly out large horizontal errors.

Results obtained using the optimization method described as follows suggest that a high-low-high thrust profile is needed. The initial high thrust would be used to increase the vehicle horizontal velocity in the desired direction. During the low thrust, or “coast” phase, the vehicle would travel a large horizontal distance without much change in velocity. The results suggest that this phase would be commanded at the lowest possible throttle setting. The final high thrust phase is used to null the horizontal velocity that was imparted to the vehicle during the first high thrust phase. A 4th and final phase, which has not been included here, would be needed for the final descent to the landing site.

### 1. Optimization Code

A Legendre Pseudospectral Method for trajectory optimization, created by Mike Ross and Fariba Fahroo of the Naval Postgraduate School, was applied to the terminal descent problem. It combines pseudospectral methods with numerical nonlinear optimization. The time domain of the trajectory is discretized at a special set of points called the Legendre-Gauss-Lobatto (LGL) points. The pseudospectral differentiation matrix is then used to transform the equations of motion from nonlinear differential equations to nonlinear algebraic equations. These equations are then posed in the form of a nonlinear programming problem, and a numerical optimizer is used to solve the problem. The method has been used on many trajectory optimization problems.<sup>9-12</sup> A short description of the method follows:

The Legendre pseudospectral differentiation matrix operates on a discrete set of points called the Legendre-Gauss-Lobatto (LGL) points. The matrix is based on Lagrange interpolation using the LGL points. A set of  $N$  LGL points are defined as follows:<sup>9</sup>

$$\begin{aligned} t_1 &= -1 \\ t_j &= \text{roots of } L'_{N-1}(t) \text{ (j=2..N-1)} \\ t_N &= 1 \end{aligned}$$

where  $L_{N-1}(t)$  is the Legendre polynomial of order  $N-1$  and  $L'_{N-1}(t)$  is the first derivative of the polynomial. These points lie in the range of  $[-1,1]$ .

It is necessary to map the real time domain to the LGL time domain by the following equation:<sup>13</sup>

$$t_{LGL_i} = \frac{2(\tau_i - \tau_o) - (\tau_f - \tau_o)}{\tau_f - \tau_o} \quad (27)$$

where  $t_{LGL_i}$  = the  $i$ th LGL time point;  $\tau_i$  = the  $i$ th real time point;  $\tau_o$  = the initial real time point;  $\tau_f$  = the final real time point.

The elements of the  $N \times N$  Legendre pseudospectral differentiation matrix ( $D_N$ ) are defined by:<sup>13</sup>

$$D_{ij} = \begin{cases} \frac{L_{N-1}(t_{LGL_i})}{L_{N-1}(t_{LGL_j})} \frac{1}{(t_{LGL_i} - t_{LGL_j})} & i \neq j \\ -\frac{N(N-1)}{4} & i = j = 1 \\ \frac{N(N-1)}{4} & i = j = N \\ 0 & \text{otherwise} \end{cases} \quad (28)$$

It is also useful to have the weights for Gaussian quadrature:<sup>13</sup>

$$w_k = \frac{2}{(N-1)N} \frac{1}{L_{N-1}^2} \quad k = 1, \dots, N \quad (29)$$

The terminal descent problem is modeled using a flat planet assumption with a constant gravitational acceleration in the vertical axis. Atmospheric effects are neglected. The equations of motion are:

$$\begin{aligned} \dot{R}_x &= V_x \\ \dot{R}_y &= V_y \\ \dot{R}_z &= V_z \\ \dot{V}_x &= a_T \cos(\theta) \cos(\beta) \\ \dot{V}_y &= a_T \cos(\theta) \sin(\beta) \\ \dot{V}_z &= a_T \sin(\theta) - g \end{aligned} \quad (30)$$

where the  $R$ 's are the position components, the  $V$ 's are the velocity components,  $a_T$  is the thrust acceleration,  $\theta$  is the thrust pitch angle from the horizontal plane, and  $\beta$  is the thrust heading angle in the horizontal plane, measured counter-clockwise from the X-axis.

It is desired to find the optimal control history of the thrust acceleration and direction angles that will minimize the required amount of propellant. The initial state and final state are specified, and the time-of-flight is free. This is equivalent to minimizing the integral of the thrust acceleration.

$$\min J = \int_{t_o}^{t_f} a_T dt \quad (31)$$

The  $D$ -matrix is used to write a discretization of the differential equations as a system of algebraic equations. After transforming the real time domain to the LGL time domain, the  $D$ -matrix is applied to (30). The equations are then rearranged into sets of equality constraints. The result is:

$$\begin{aligned} \vec{C}_{\dot{R}_x} &= D_N \vec{R}_x - \frac{(\tau_f - \tau_o)}{2} [\vec{V}_x] = 0 \\ \vec{C}_{\dot{R}_y} &= D_N \vec{R}_y - \frac{(\tau_f - \tau_o)}{2} [\vec{V}_y] = 0 \\ \vec{C}_{\dot{R}_z} &= D_N \vec{R}_z - \frac{(\tau_f - \tau_o)}{2} [\vec{V}_z] = 0 \\ \vec{C}_{\dot{V}_x} &= D_N \vec{V}_x - \frac{(\tau_f - \tau_o)}{2} [\vec{a}_T \cos(\vec{\theta}) \cos(\vec{\beta})] = 0 \\ \vec{C}_{\dot{V}_y} &= D_N \vec{V}_y - \frac{(\tau_f - \tau_o)}{2} [\vec{a}_T \cos(\vec{\theta}) \sin(\vec{\beta})] = 0 \\ \vec{C}_{\dot{V}_z} &= D_N \vec{V}_z - \frac{(\tau_f - \tau_o)}{2} [\vec{a}_T \sin(\vec{\theta}) - g] = 0 \end{aligned} \quad (32)$$

where each vector represents the value of the discretized states and controls at each LGL point. The C's are vectors of constraints that must be met at each LGL point.

The objective function to minimize the integral of the thrust acceleration becomes:

$$\min J = \frac{(\tau_f - \tau_o)}{2} \vec{w}^T \vec{a}_T \quad (33)$$

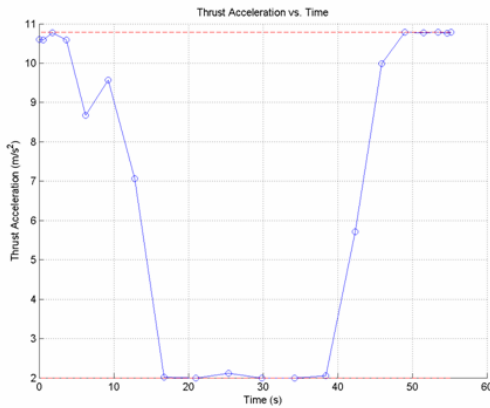
The optimization vector for the parameter optimization problem is:

$$\vec{x}_{opt} = \begin{bmatrix} \vec{R}_x \\ \vec{R}_y \\ \vec{R}_z \\ \vec{V}_x \\ \vec{V}_y \\ \vec{V}_z \\ \vec{a}_T \\ \vec{\theta} \\ \vec{\beta} \\ \tau_f \end{bmatrix}$$

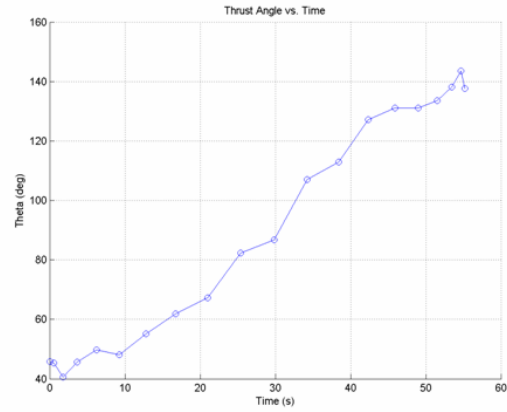
Lower and upper bounds are placed on the optimization vector so that the initial and final states are fixed. Upper and lower limits are also placed on the thrust acceleration.

## 2. Results

Figure 11 shows a sample commanded acceleration profile for a stress case that flies 4 km in range over only 1.5 km for altitude change. Note the high-low-high thrust command as discussed earlier. The minimum and maximum acceleration was limited in this case to 2.0-10.78 m/s<sup>2</sup>. The maximum limit roughly corresponds to T/W of 1.1 (in Earth G). The minimum limit is about 18.5% of the max thrust and is based on the Mars Science Laboratory (MSL) configuration as of mid-2004. Figure 11 also shows the thrust angle variation with time. Note a roughly linear relationship with time.



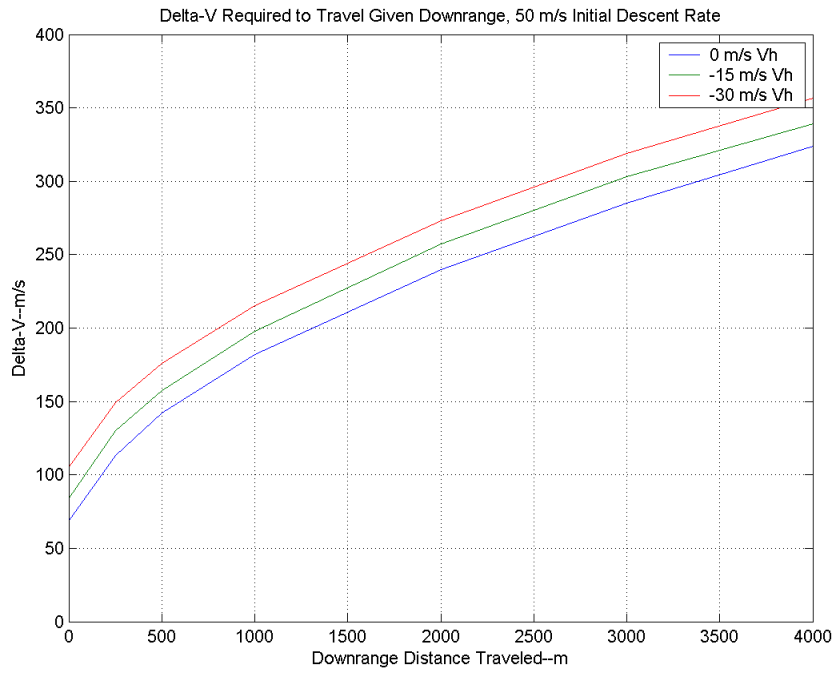
(a) Thrust Acceleration



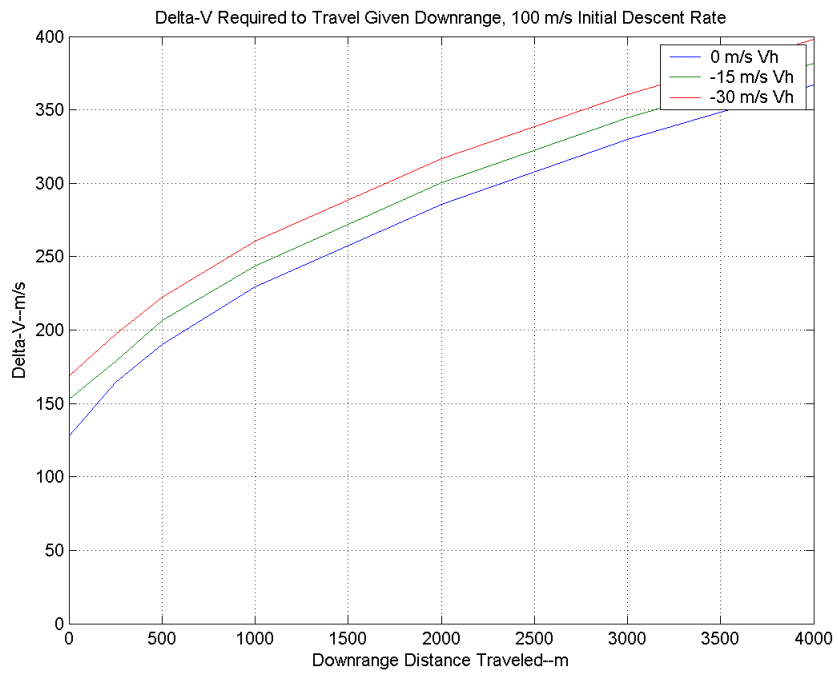
(b) Thrust Angle

**Figure 11. Sample Commanded Profile Using Legendre Pseudospectral Method**

Figure 12 shows the amount of delta-V required to fly various divert distances using this scheme. The cost increases with divert distance. Figure 12(a) shows the delta-V needed for an initial descent rate of 50 m/s, and the 100 m/s data is shown in figure 12(b). The different curves correspond to an initial horizontal velocity, shown in the legend. The horizontal velocities are in the opposite direction as that of the divert. The start altitude is optimized for each case. The highest engine start altitude for the 50 m/s cases is 1.6 km, and the longest burn is 60 sec. For the 100 m/s cases, the highest start altitude is 2.7 km and the longest burn is just under 60 sec.



(a) 50 m/s Descent Rate



(b) 100 m/s Descent Rate

Figure 12. Divert Delta-V Requirement

The kinds of initial conditions used for these runs are likely to be encountered for robotic missions in which a parachute has been used to slow the majority of the horizontal velocity, and the remaining velocity is mostly vertical. The results show the cost of providing the capability to solve the remaining position error from the entry phase and wind drift. For example, a 1000-kg landed mass with a terminal parachute sized to a 50 m/s descent rate would require 34 kg of propellant in the best case scenario (assuming  $I_{sp} = 210$  sec). However, if the mission required capability for up to 4 km of divert and 30 m/s horizontal velocity in the wrong direction, this would cost 189 kg of propellant. This is an increase of 155 kg of propellant, without considering margin. This extra propellant must be carried from launch and would have a large impact on the overall mission design. The cost of diverting during powered descent is significant and should be minimized as much as possible by improvements in accuracy during the entry phase. Steerable parachutes may also help increase accuracy by minimizing wind drift and should be considered for pinpoint missions.

To show the improvement this type of scheme has over previously considered schemes, the data is compared to the old MSL guidance<sup>14</sup> in figure 13. The initial conditions are a 50 m/s descent rate and zero horizontal velocity. The blue curve represents the optimal solutions. The green curve is the  $\Delta V$  required using the old MSL guidance, which employs a restricted quadratic scheme. The  $\Delta V$  increases as divert distance increases. For the small divert cases, the MSL guidance and optimal solutions are close in magnitude. As divert increases, the optimal solution performs much better. The old MSL guidance solution was designed with capability for small divert distances in mind ( $< 200$  m), not for large, pinpoint class divert requirements.

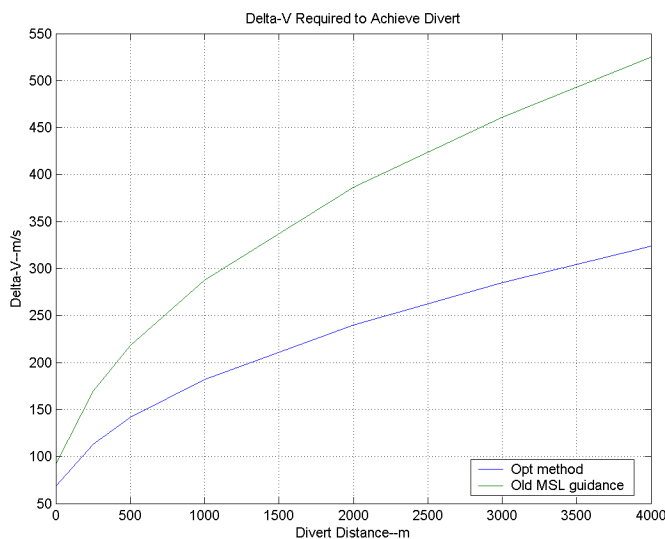


Figure 13. Comparison of old MSL Guidance to Optimal Solution

## Conclusion

A combination of different methods for powered descent guidance should be pursued, depending on the application. At the Moon, the braking phase must be at or near optimal due to the large amount of delta-V necessary to slow the vehicle from orbit. Two-pt boundary value methods with proper targeting may prove to be adequate, but more advanced methods should be pursued. For the succeeding phases, two-pt boundary value methods are sufficient. At Mars, the potential range of initial conditions for the terminal phase can vary widely depending on the mission. Parachutes are typically used for robotic missions but a chute system may not be feasible for the more massive human missions, which would lead to higher initial velocities and a greater delta-V requirement for the propulsive phase. In addition, with current state-of-the-art Entry, Descent, and Landing, a large downrange change during the propulsive phase may be necessary and must be accounted for in the vehicle design. Optimal methods must be pursued for these pinpoint cases but two-pt boundary value methods should remain available for less stressful mission requirements or phases.

## Appendix

### Propellant Mass

Throughout this paper, the main performance measure cited is delta-V, since it is a more general performance index and can be applied to any size vehicle. However, a more tangible measure of the performance is the propellant mass required to perform the trajectory maneuvers. The amount of mass change during the maneuver is related to the delta-V via the rocket equation, the derivation of which is commonly found in many aerospace texts.

$$\frac{M_0}{M_f} = e^{\Delta V / g_0 I_{sp}} \quad (34)$$

The propellant mass required,  $M_p$ , is the difference between the initial mass,  $M_0$ , and the final mass,  $M_f$ .

$$M_p = M_0 - M_f \quad (35)$$

Figure 14 shows the amount of propellant mass required for a 1000-kg vehicle given a particular delta-V and  $I_{sp}$ . Each curve represents a different value of  $I_{sp}$ , as shown in the legend.

As seen in equation (34), the result of the rocket equation is a mass ratio. Thus, the data in figure 14 is easily scalable to any size vehicle, by multiplying the amount of propellant read from the figure by the vehicle mass and then dividing by the reference 1000-kg mass.

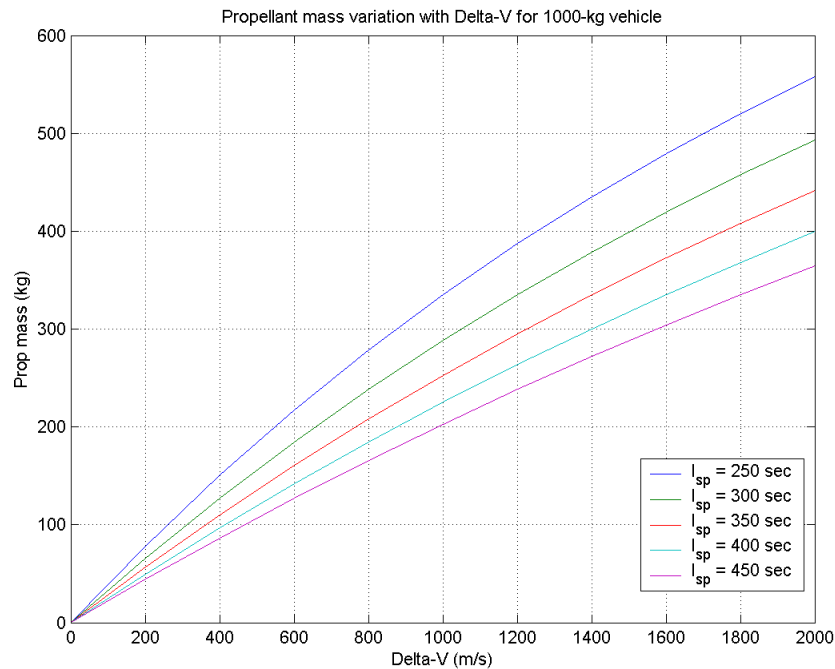


Figure 14. Propellant Mass

### Acknowledgments

Thank you to Lee Bryant for serving as technical reviewer, and also for advice and guidance during this study.

Thank you to the Aeroscience and Flight Mechanics Division for support in allowing us to perform and present this work.

## References

- <sup>1</sup>Condon, Jerry; presentation entitled "First Lunar Outpost Powered Descent Design and Performance", NASA JSC Systems Engineering Division, Performance Analysis Branch; September 14, 1992.
- <sup>2</sup>Klumpp, Allan R., "Apollo Lunar-Descent Guidance", Charles Stark Draper Laboratory, R-695, June 1971.
- <sup>3</sup>Bryson, A.E., Ho, Y., *Applied Optimal Control*, Ginn, Waltham, 1969.
- <sup>4</sup>Jaggers, Roland F., "Shuttle Powered Explicit Guidance (PEG) Algorithm", Rockwell Space Operations Company, November 1992, JSC-261 22.
- <sup>5</sup>Ingoldby, R. N. (Martin Marietta Aerospace, Denver, Colo.), "Guidance and control system design of the Viking planetary lander", AIAA-1977-1060; Guidance and Control Conference, Hollywood, Fla., August 8-10, 1977, Technical Papers. (A77-42751 20-35) New York, American Institute of Aeronautics and Astronautics, Inc., 1977, p. 164-171.
- <sup>6</sup>Viking Lander System Primary Mission Performance Report, Martin Marietta Corporation (Denver, CO), April 1977, NASA CR-145148.
- <sup>7</sup>Mendeck, G., Carman, G., "Apollo-Derived Entry Guidance for Mars Smart Landers (AIAA-2002-4502)," AIAA Atmospheric Flight Mechanics Conference, Monterey, CA, August 2002.
- <sup>8</sup>Crain, T., Bishop, R., "Mars Entry Navigation: Atmospheric Interface Through Parachute Deploy (AIAA-2002-4501)," AIAA Atmospheric Flight Mechanics Conference, Monterey, CA, August 2002.
- <sup>9</sup>Fahroo, F. and Ross, I. M., "A Spectral Patching Method for Direct Trajectory Optimization," *The Journal of the Astronautical Sciences*, Vol. 48, No. 2/3, 2000.
- <sup>10</sup>Ross, I. M. and Fahroo, F., "A Direct Method for Solving Nonsmooth Optimal Control Problems," *Proceedings of the International Federation on Automatic Control, 15th World Congress*, Barcelona, Spain, July 2002.
- <sup>11</sup>Ross, I. M. and Fahroo, F., "User's Manual for DIDO 2001: A MATLAB Application Package for Dynamic Optimization", NPS Technical Report AA-01-003, Department of Aeronautics and Astronautics, Naval Postgraduate School, Monterey, California, June 2001.
- <sup>12</sup>Rea, J., "Launch Vehicle Trajectory Optimization Using a Legendre Pseudospectral Method (AIAA-2003-5640)," AIAA Guidance, Navigation, and Control Conference and Exhibit, Austin, Texas, August 2003.
- <sup>13</sup>Fahroo, F. and Ross, I. M., "Costate Estimation by a Legendre Pseudospectral Method," *Journal of Guidance, Control and Dynamics*, Vol. 24, No. 2, Mar.-Apr. 2001, pp. 270-277.
- <sup>14</sup>Wong, E., Masciarelli, J., and Singh, G., "Autonomous Guidance and Control Design for Hazard Avoidance and Safe Landing on Mars", AIAA Paper 2002-4502, Atmospheric Flight Mechanics Conference, Monterey, CA, August 2002.